Korean J. Chem. Eng., 34(4), 1177-1186 (2017)
DOI: 10.1007/s11814-017-0010-8

pISSN: 0256-1115
eISSN: 1975-7220

Removal of anionic dyes from aqueous solutions using polyacrylamide and polyacrylic acid hydrogels

Khadijeh Didehban†, Mozhgan Hayasi, and Fatemeh Kermajani

Department of Chemistry, Payame Noor University, Tehran, P. O. Box 19395-36972, Iran
(*Received 19 April 2016 • accepted 2 February 2017*)

Abstract−This study deals with the application of polyacrylamide (PAM) and polyacrylic acid (PAA) hydrogels in the removal of anionic dyes such as reactive orange-20 (RO-20) and direct red-31(DR-31) from aqueous solutions. The adsorption efficiency of as-prepared hydrogels was compared with each other and the suitable hydrogel for adsorption of RO-20 and DR-31 dyes was identified. Adsorption experiments were performed as function of pH, PAM or PAA dosage, contact time and initial dyes concentration. Langmuir and Freundlich isotherm models were used to describe the equilibrium adsorption data. The results displayed that the adsorption data fitted with Langmuir model more than Freundlich model for DR-31 and fitted well with Freundlich model for RO-20. The kinetic studies showed that the experimental data fitted well with the pseudo-second order kinetic model. This study showed that PAM could be used as effective adsorbent for removal of anionic dyes in comparison with PAA.

Keywords: Anionic Dyes, Polyacrylamide, Polyacrylic Acid, Hydrogel, Adsorption

INTRODUCTION

Dye contamination in wastewater due to the industrial activities such as petroleum, textile, paper and plastic has become a serious environmental problem. The discharge of dyes in the environment damages to natural ecosystems, because most of dyes are toxic, allergenic, potentially carcinogenic and mutagenic [1,2]. Therefore, it is necessary to eliminate toxic dyes from industrial effluents before their discharge into the environment. Numerous methods such as electrochemical treatment, adsorption, coagulation, chemical oxidation and membrane processes have been applied to eliminate dyes from wastewaters [3,4]. Among these methods, adsorption has been established to be an effective technique for removal of dyes from wastewaters because of its low costs, simple design, no secondary pollution and high efficiency [5,6]. Many different adsorbents ,such as activated carbon, flay ash, clay, polymeric materials, carbon nanotubes, zeolite, have been widely used for dye removal from aqueous solution [7-11]. Among the adsorbents, polymeric materials especially polymeric hydrogels have attracted much attention in the wastewaters treatment because of their unique properties [12-14].

Hydrogels are crosslinked hydrophilic polymers with three-dimensional structure which can absorb large amounts of water or other aqueous solutions without dissolving because of their crosslink network [15]. These hydrophilic polymers possess functional groups such as NH_2, COOH, OH etc., which can be used for selective adsorption of various dyes from wastewater. Acrylic acid and acrylamide monomers have been recognized as most common materials for manufacturing of polymeric hydrogels [16,17]. Polyacrylamide (PAM) is a soluble polymer in water, has amide (-$CONH_2$) groups which act as active sites for removal of dyes from aqueous solution, also it has good stability and good mechanical strength [18,19]. Polyacrylic acid (PAA) is a hydrophilic and inexpensive polymer, has good resilience and high respond to external stimuli such as pH [20]. Therefore, many attempts have been made to manufacture the hydrogels based on the polyacrylamide and polyacrylic acid hydrogels [21-23].

There are some recent reports on removal of dyes by hydrogels, for example Bhattacharyya et al. synthesized poly(acrylamide-co-hydroxyethylmethacrylate) hydrogels and used these hydrogels for removal of rhodamine B and crystal violet dyes from wastewater [24]. poly(acrylic acid-acrylamide) hydrogels were used in crystal violet and basic magenta removal [23]. Poly(methacrylate-acrylic acid-vinyl acetate) [25] and polyacrylamide/cellulose nanocrystal nanocomposite hydrogels [26] were prepared and used for methylene blue removal. Hydrogels based on polyethylene glycol and polyacrylic acid were used for adsorption of congo red and crystal violet dye from aqueous solution [27] etc. To the best of our knowledge, polymeric hydrogels based on PAM and PAA have not been used for removal of DR-31 and RO-20 dye so far.

We prepared PAA and PAM hydrogels, then used the resultant hydrogels for removal of reactive orange-20 and direct red-31 dye from water. The objectives of this work were to identify the suitable hydrogel for adsorption of DR-31 and RO-20 dye and to compare the adsorption efficiency of as-prepared hydrogels. We studied the effects of four variables such as adsorbent dosage, pH value of prepared solution, adsorption time and dye concentration on the adsorption of dyes. Adsorption kinetics and isotherm models for DR-31 and RO-20 removal onto as-prepared hydrogels were also investigated.

†To whom correspondence should be addressed.
E-mail: kh_didehban@yahoo.com

EXPERIMENTAL

1. Materials

Acrylamide (AM) monomer, potassium persulfate (KPS) as initiator, Acrylic acid (AA) monomer, N,N-methylene-bis-acrylamide (MBA) as crosslinker, hydrochloric acid solution (HCl, 36-38%), N,N,N′,N′-tetramethylethylenediamine (TEMED) and sodium hydroxide (NaOH) were obtained from Merck Chemical Co. Reactive orange-20 (RO-20) (solubility, >100 g/L at 25 °C) and direct red-31 (DR-31) dye (solubility, 45 g/L at 80 °C) were supplied by Win-Chem, which their molecular structures are shown in Fig. 1.

2. Synthesis of Polyacrylamide and Polyacrylic Acid Hydrogels

Free radical cross-linking polymerization was performed for synthesis of hydrogels based on PAM and PAA in aqueous solution. To prepare the PAM hydrogel, AM monomer (1 g) and MBA crosslinker (0.06 g) were dissolved in distilled water (15 mL) and stirred vigorously. The solution was purged with nitrogen gas, and then KPS initiator (0.1 g) was added into the solution, after dissolving of initiator, 50 µl of TEMED was added to the system. After a short time, the PAM hydrogel was formed and the reaction was continued for another 2 h at room temperature to complete the polymerization.

To prepare the PAA hydrogel, 2 ml of AA monomer was dissolved in distilled water (31 mL) and stirred, then 0.06 g of MBA crosslinker was added and the mixture solution was transferred to the flask equipped with a reflux condenser. Then, the crosslinker was dissolved completely, KPS initiator (0.1 g) and TEMED (50 µl) were added to the solution. When the temperature was raised to 58 °C, the hydrogel was formed and the polymerization reaction was continued for another 2 h at 58 °C under nitrogen flow. The obtained hydrogels were washed with distilled water and dried at room temperature.

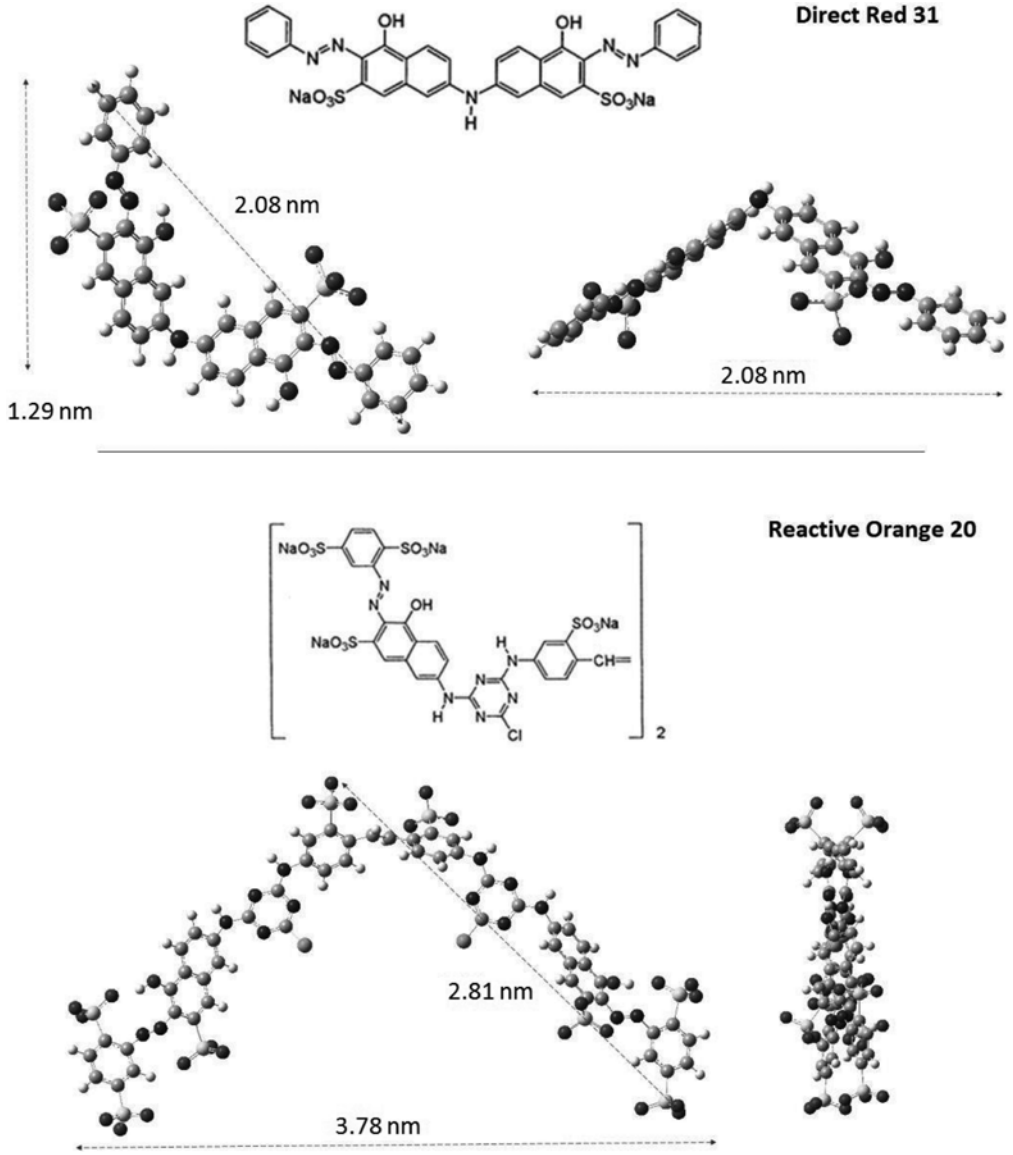

Fig. 1. Molecular structure and optimized three-dimensional structural formulae of RO-20 and DR-31 dyes. The dimensions of the dyes were calculated using Hyper Chem version 8.0.10.

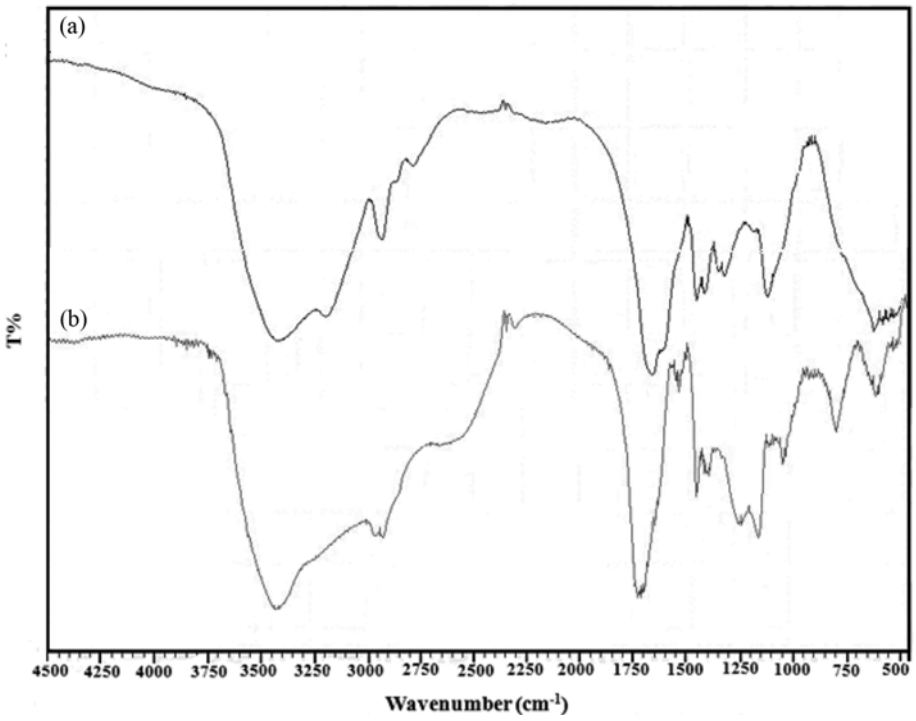

Fig. 2. FT-IR spectra of PAM (a) and PAA (b) hydrogels.

3. Characterization

Fourier-transform infrared (FTIR) spectra of hydrogels were analyzed using an FTIR-8101M Shimadzu spectrometer with KBr pellet in the region of 400-4,000 cm^{-1} to investigate the chemical structures of synthesized samples. The thermogravimetric analysis (TGA) of PAM, PAA and poly(AA-co-AM) hydrogels was determined by STA-1500 analyzer at the scanning rate of 10 °C/min in air atmosphere. Scanning electron microscopy (SEM) was used to observe the morphologies of hydrogels and dye-loaded hydrogels and carried out by AIS 2100 scanning electron microscope. The concentrations of RO-20 and DR-31 dyes were measured using a Sentry 20 UV-Visible spectrophotometer at λmax=346 nm (RO-20) and λmax=523 nm (DR-31).

4. Adsorption Experiments

Adsorption experiments of DR-31 and RO-20 were performed at 25 °C, in a shaker with a speed of 150 rpm, in batch conditions. To investigate the effect of pH on dyes adsorption and to determine the optimal pH, 0.1 g of hydrogels were mixed with 50 mL of dyes solution (50 mg L^{-1}) separately and the pH of the DR-31 and RO-20 solutions was adjusted from 1.0 to 8.0. The effect of hydrogels dosages on adsorption of dyes was studied by mixing of 50 mL of 50 mg/L solutions of dyes with different amounts of hydrogels (0.05-0.6 g). The effect of RO-20 and DR-31 concentrations was studied by contacting 50 mL of dyes solutions with various concentrations from 25 to 150 mg L^{-1}. The amount of RO-20 and DR-31 adsorbed on the hydrogels (q) was evaluated according to the following equation (Eq. (1)):

$$q=(C_0-C_e)V/m \quad (1)$$

The percentage of dyes removal (R) was determined according to Eq. (2):

$$R=(C_0-C_e)/C_0\times100\% \quad (2)$$

where C_0 is the initial and C_e is the equilibrium concentrations of RO-20 and DR-31 dyes in the solution (mg L^{-1}), q (mg g^{-1}) is the amount of adsorbed dyes per gram of hydrogels, m is the mass of the used hydrogels (g) and V (L) is the volume of the RO-20 or DR-31 solution.

RESULTS AND DISCUSSION

1. Characterization of Synthesized Hydrogels

The structural characteristics of synthesized hydrogels were studied by FTIR. Fig. 2 shows the FTIR spectra of PAM, PAA and poly (AA-co-AM) hydrogels. According to the spectrum of PAM, the peaks at 1,454 cm^{-1} and 1,658 cm^{-1} are related to the C-N stretching and C=O stretching of amide, respectively. The absorption peaks around 1,614 cm^{-1} and 3,412 cm^{-1} correspond to N-H bending and N-H stretching of acrylamide. PAA exhibited peaks at 1,716, 1,049 and 1,165 cm^{-1}, corresponding to the C=O, C-O and -CO-O- stretching of acrylic acid; also the peak observed at 3,429 cm^{-1} is assigned to O-H stretching. In the FTIR spectra of all hydrogels, the peaks in the range of 2,860-2,900 cm^{-1} are attributed to the C-H stretching of polymers.

The thermal stability of the synthesized hydrogels was examined by TGA. The results of TGA for hydrogels are represented in Fig. 3. The thermal degradation of PAM hydrogel occurred in three weight loss regions: the first weight loss between 50 and 208 °C was attributed to the loss of physically adsorbed and interlayer water, and it was about 10 wt%; the decomposition of functional groups

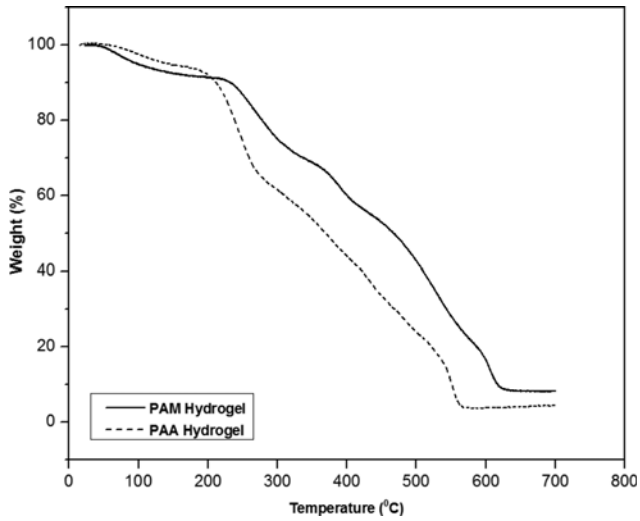

Fig. 3. Thermogravimetric curves of PAM and PAA hydrogels.

occurred in the region of 220-360 °C with the weight loss of 21 wt%; the major weight loss (60 wt%), which was observed between 362 and 618 °C, can be due to the degradation of PAM chains' backbone. The weight loss pattern of PAA was similar to the PAM and the PAA decomposed in three stages. The first stage with 5 wt% weight loss was in the range of 70-160 °C. The second stage was between 175 and 263 °C (25 wt% weight loss), and the degradation of PAA chains' backbone occurred in the temperature region of 270-560 °C with weight loss of about 61 wt%. The results indicated that the thermal stability of PAM hydrogel was higher than the thermal stability of PAA hydrogel.

The morphologies of synthesized hydrogels and dye-loaded hydrogels were examined by SEM. Figs. 4 and 5 display the SEM micrographs of hydrogels before and after adsorption of dye. As can be seen, the PAM hydrogel has almost a smooth surface with a regular and homogeneous morphology, which may be attributed to the crosslinking polymer network (Fig. 4(a), (b)), while PAA hydrogel has a rather irregular morphology with little cavities (Fig. 5(a), (b)). It was found that the surface of hydrogels became wrinkled and coarser after adsorption of dye. Thus, difference between the morphologies of hydrogels and dye-loaded hydrogels confirms the adsorption of dyes onto hydrogels.

Textural properties of the PAM and PAA hydrogels were characterized by Brunauer-Emmett-Teller (BET) method. The BET analysis was carried out by N_2 physisorption using a porosimeter (BEL Japan, Inc.). Fig. 6(a), (b) shows the N_2 adsorption-desorption isotherms and the corresponding pore size distribution of hydrogels obtained by Barrett-Joyner-Halendar (BJH) method. As seen in Fig. 6(a), both of hydrogels show similar behavior to those of type IV, which indicates the presence of mesopores in hydrogels but in PAA, the size distribution continued into the macropore domain. Table 1 presents the specific surface area, pore volume and pore size of hydrogels. PAM hydrogel had higher surface area compared to the PAA hydrogel, but the pore size and pore volume of PAM hydrogel were smaller than those of PAA hydrogel. Although PAM had smaller pore size and pore volume, its adsorption capacity was larger than that of PAA hydrogel. Thus, it could be inferred that the interactions between functional groups of adsorbent and dyes molecules occurred on the surface of hydrogels,

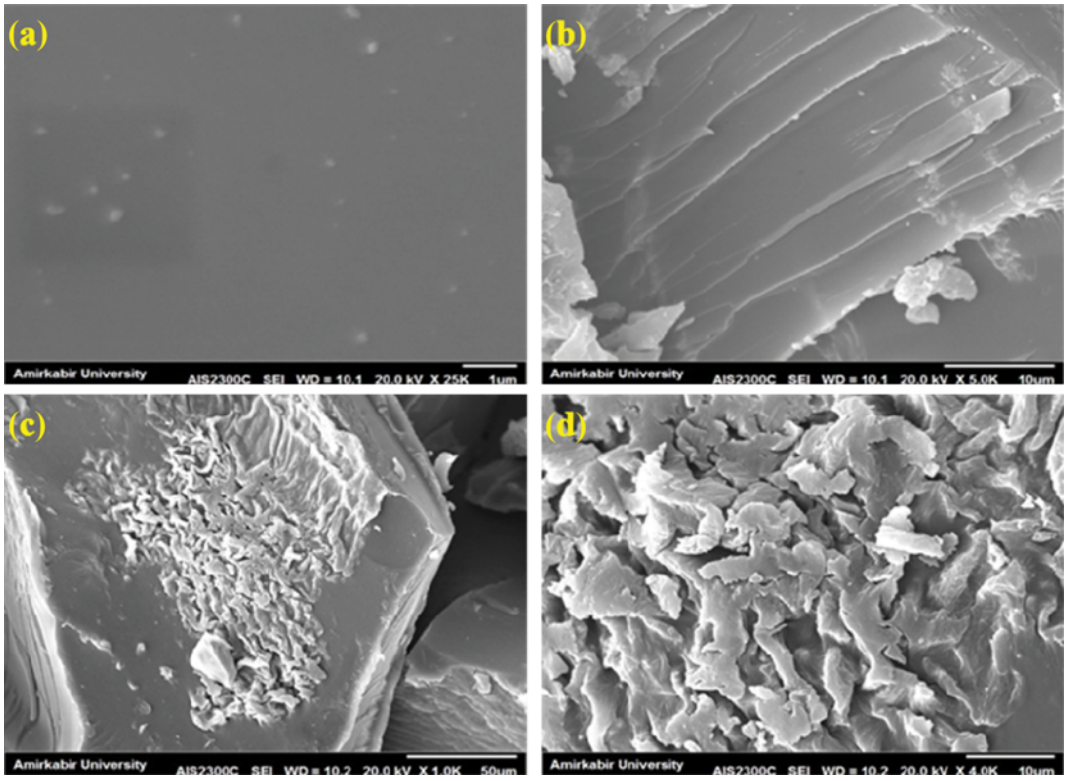

Fig. 4. SEM images of PAM hydrogel (a), (b) PAM hydrogel after dye adsorption (c), (d).

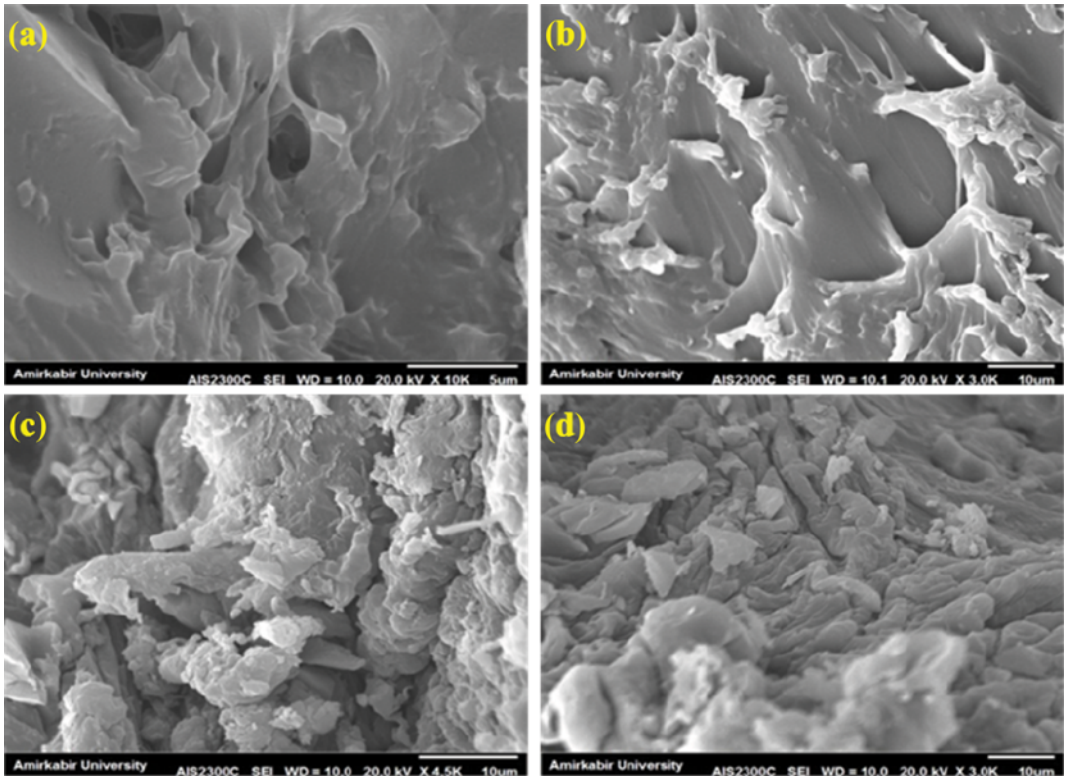

Fig. 5. SEM images of PAA hydrogel (a), (b) PAA hydrogel after dye adsorption (c), (d).

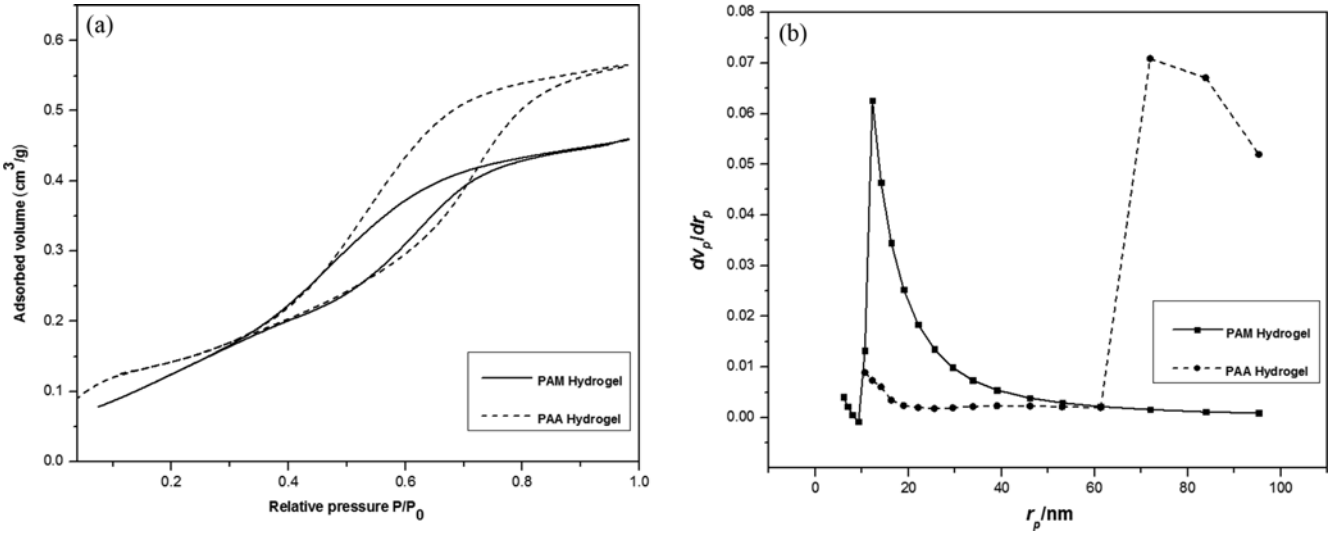

Fig. 6. The N_2 adsorption-desorption isotherms (a) and the pore size distributions (b) of PAM and PAA hydrogels.

Table 1. The structure parameters of PAM and PAA hydrogels

Hydrogel	BET specific surface area (m^2/g)[a]	Pore volume (cm^3/g)[b] Vp	Pore size (nm)[b]
PAM	1.31	0.00058	12.24
PAA	0.639	0.00211	71.9

[a]Determined by BET method
[b]Determined by BJH method

and the active sites inside of the pore were not well accessible to the dyes molecules.

2. Effect of Operational Parameter on Dye Removal

2-1. Effect of pH on Adsorption of RO-20 and DR-31 Dyes

The effect of pH on the adsorption capacity of RO-20 or DR-31 dyes onto PAM and PAA hydrogels was evaluated and illustrated in Fig. 7. As shown, the amount of adsorbed dyes onto the hydrogels decreased with the increasing of pH value. The maximum

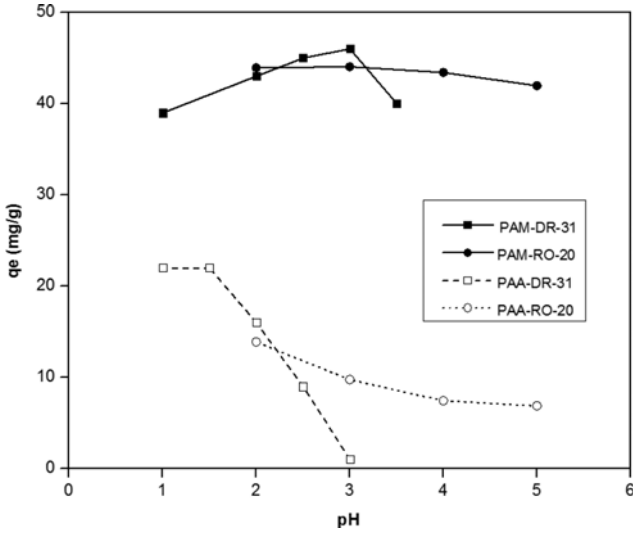

Fig. 7. Effect of pH on the adsorption of RO-20 and DR-31 onto PAM and PAA hydrogel.

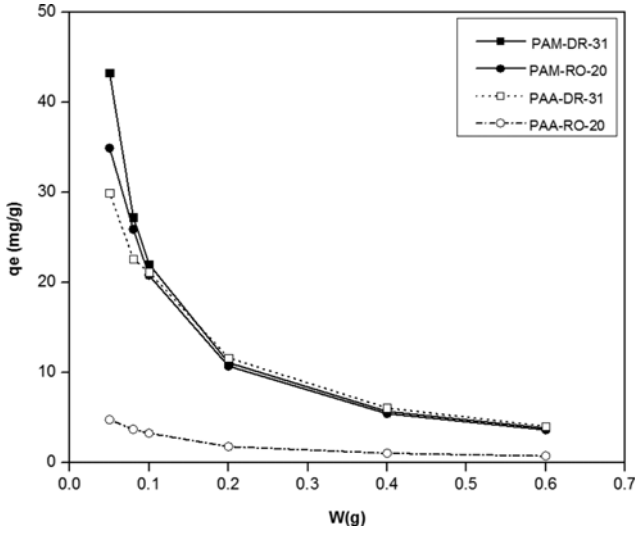

Fig. 8. Effect of adsorbent dosage on the removal of RO-20 and DR-31 onto PAM and PAA hydrogel.

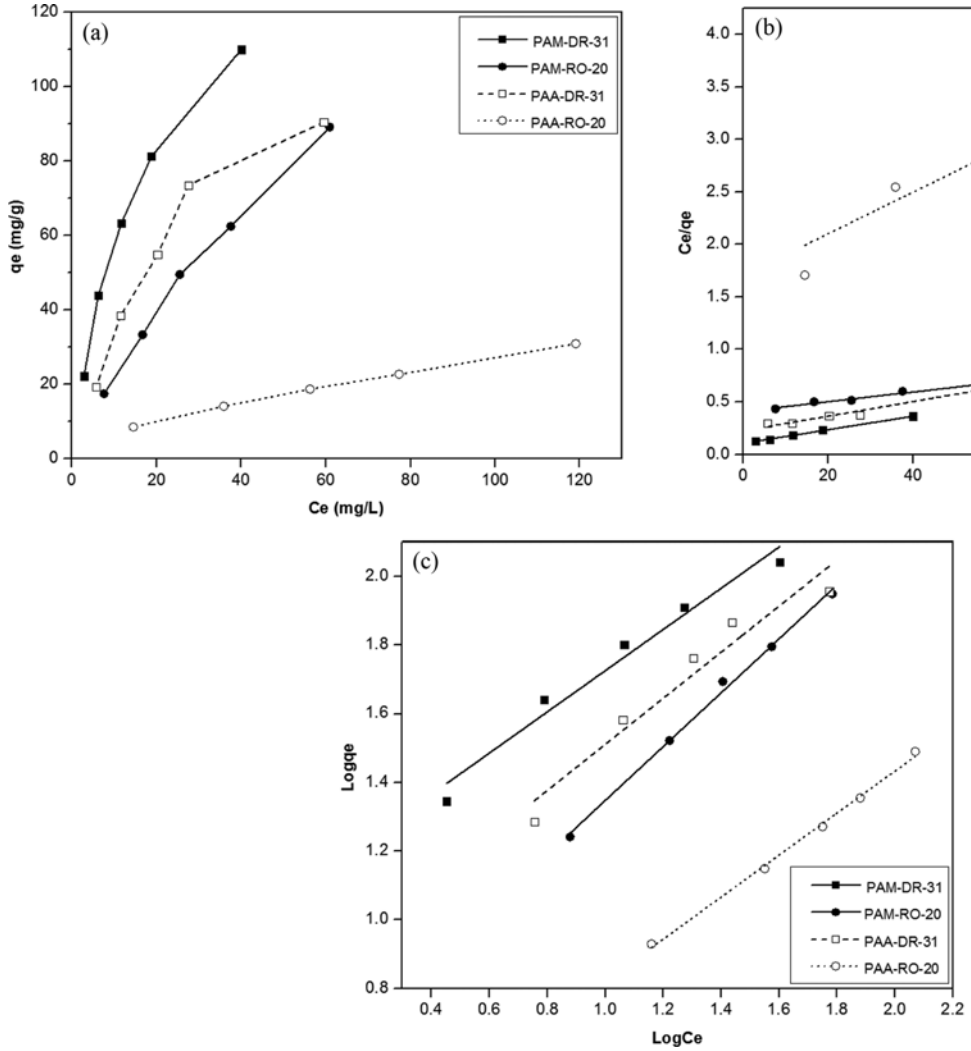

Fig. 9. Effect of dye concentration on the removal of RO-20 and DR-31 by PAM and PAA (a), the equilibrium isotherm for RO-20 and DR-31 adsorbed by PAM and PAA, Langmuir isotherm (b), the Freundlich isotherm (c).

adsorption of RO-20 onto PAM hydrogel and PAA hydrogel occurred at pH 3 and pH 2, respectively, and the maximum adsorption of DR-31 onto PAM hydrogel and PAA hydrogel occurred at pH 3 and pH 1.5, respectively. In an acidic pH solution, the functional groups of hydrogels are protonated and the surface of hydrogels becomes positively charged. Thus, electrostatic interaction develops between the adsorbents and the negatively charged RO-20 or DR-31 dye, leading to the increase in the adsorption capacity of dyes. On the contrary, at high pH, the adsorption capacity of dyes decreases, because the numbers of negatively charged sites of adsorbents increases, resulting in the electrostatic repulsion between dyes and adsorbents. Thus, the adsorption experiments were conducted at acidic pH in further studies.

2-2. Effect of Adsorbent Dosage

To investigate the effect of adsorbent dosage on RO-20 and DR-31 dyes adsorption, different dosages of hydrogels ranging between 0.05 and 0.6 g were used. As can be seen from Fig. 8, the amount of adsorbed RO-20 or DR-31 dye decreases with the increase in the adsorbents dosage. The decrease in adsorption capacity might be ascribed to the increase in the ratio of active sites of hydrogels to the dye molecules, which resulted in the unsaturation of active sites [28].

2-3. Effect of Dye Concentration and Adsorption Isotherms

The variations of RO-20 and DR-31 adsorption onto the PAM and PAA hydrogels with feed concentration of dyes solution are

Table 2. Isotherm parameters for the adsorption of DR-31 and RO-20 onto PAM and PAA hydrogels

Samples	Langmuir			Freundlich		
	q_m (mg/g)	K_L (L/mg)	R^2	K_F ($mg^{1-(1/n)}$ $L^{1/n}$)/g	1/n	R^2
PAM-DR-31	155.279	0.060	0.997	13.335	0.599	0.961
PAM-RO-20	216.919	0.011	0.968	9.867	0.785	0.995
PAA-DR-31	143.884	0.031	0.953	6.915	0.671	0.924
PAA-RO-20	50.582	0.0115	0.898	1.621	0.612	0.996

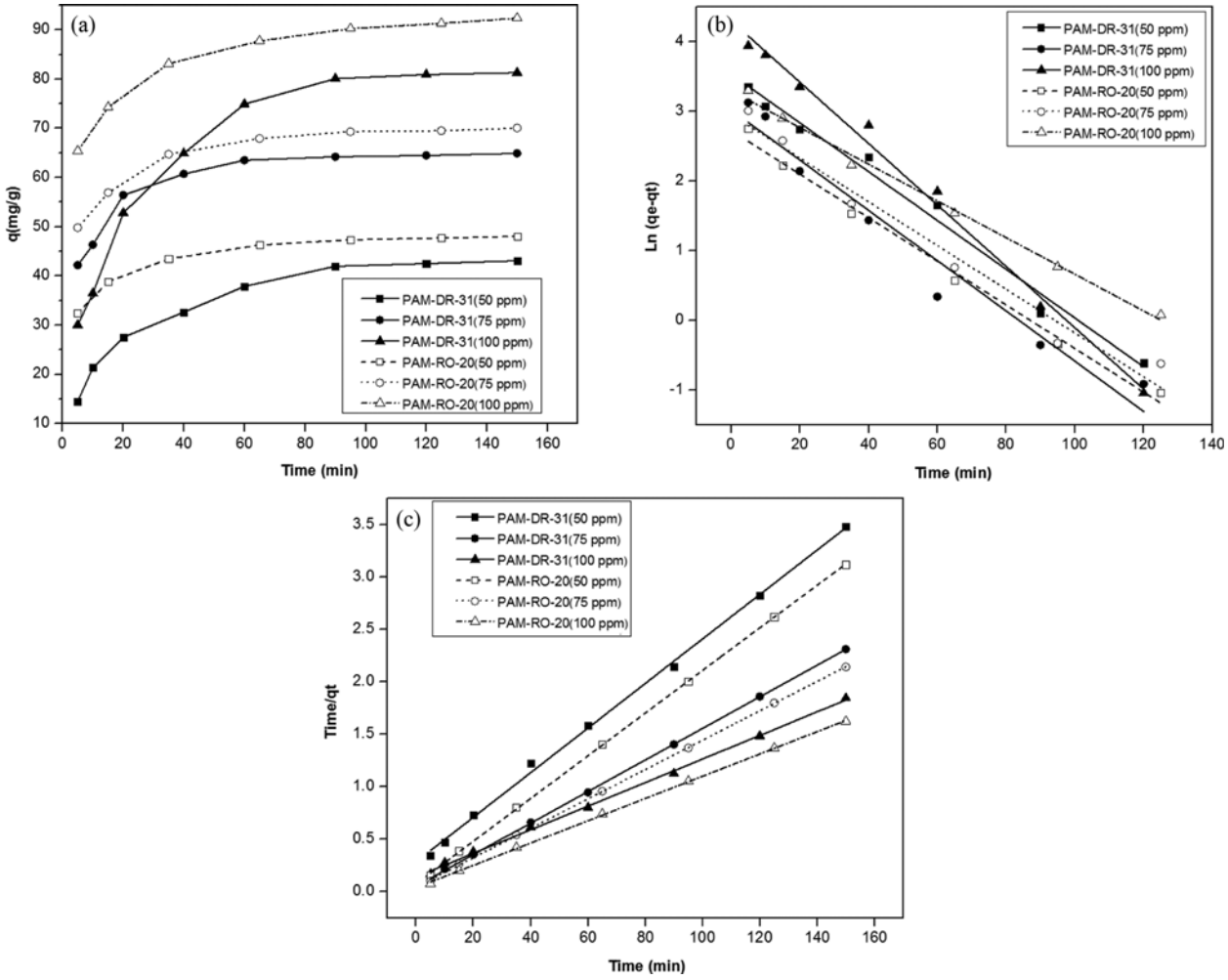

Fig. 10. Effect of contact time on the removal of DR-31 and RO-20 by PAM (a), pseudo-first-order model (b) pseudo-second-order model (c).

shown in Fig. 9(a). As seen, the amount of adsorbed dyes onto adsorbents increases with an increase in initial RO-20 and DR-31 dye concentration. This may be due to the increase in the driving force of the initial dyes concentration, which overcomes the mass transfer resistance. To understand the mechanism of the adsorption, two commonly isotherm models, Langmuir and Freundlich, were applied to determine the isotherm parameters [29,30]. The Freundlich isotherm model assumes multilayer adsorption onto heterogeneous surface of hydrogels absorbents, which is represented by the following equation:

$$q_e = K_F C_e^{1/n} \quad (3)$$

Conversely, the Langmuir isotherm is applied to monolayer adsorption onto homogeneous surface, with finite number of active sites. This model is expressed by the following equation:

$$q_e = \frac{q_m K_L C_e}{1 + K_L C_e} \quad (4)$$

where q_e (mg/g) is the equilibrium adsorption capacity, n is the heterogeneity factor, K_F (L/mg) is the Freundlich constant, C_e (mg/L) is the equilibrium dye concentration, q_m (mg/g) is the maximum capacity of the adsorbent and K_L (L/mg) is the Langmuir constant. Table 2 presents the adsorption isotherm parameters obtained from Langmuir and Freundlich models. The Langmuir and Freundlich isotherm parameters could be obtained by plotting C_e/q_e versus C_e and Log q_e versus Log C_e, respectively, and determined from the slope and the intercept of plots. According to the results, the adsorption capacities of dyes onto PAM hydrogel are higher than those of PAA hydrogel. This may be related to the presence of amide groups of the PAM hydrogel, which has strong interaction with functional groups of RO-20 and DR-31 molecules. Between the two polymers, the pKa value of PAM is higher than that of PAA [31,32], so under acidic conditions, the amide groups of PAM can be easily protonated compared to the carboxylic groups of PAA, resulting in the increase of positive charges on the surface of PAM. Thus, a strong electrostatic interaction happens between functional groups of PAM and the sulfonate groups of the anionic dye molecules. Also, PAM has higher specific surface area compared to PAA, so it can adsorb more dye molecules. Fig. 9(b), (c) shows the linear fitting of Langmuir and Freundlich isotherm models; as seen the Langmuir model fit better than Freundlich model for DR-31 dyes, suggesting that a monolayer adsorption of DR-31 dye

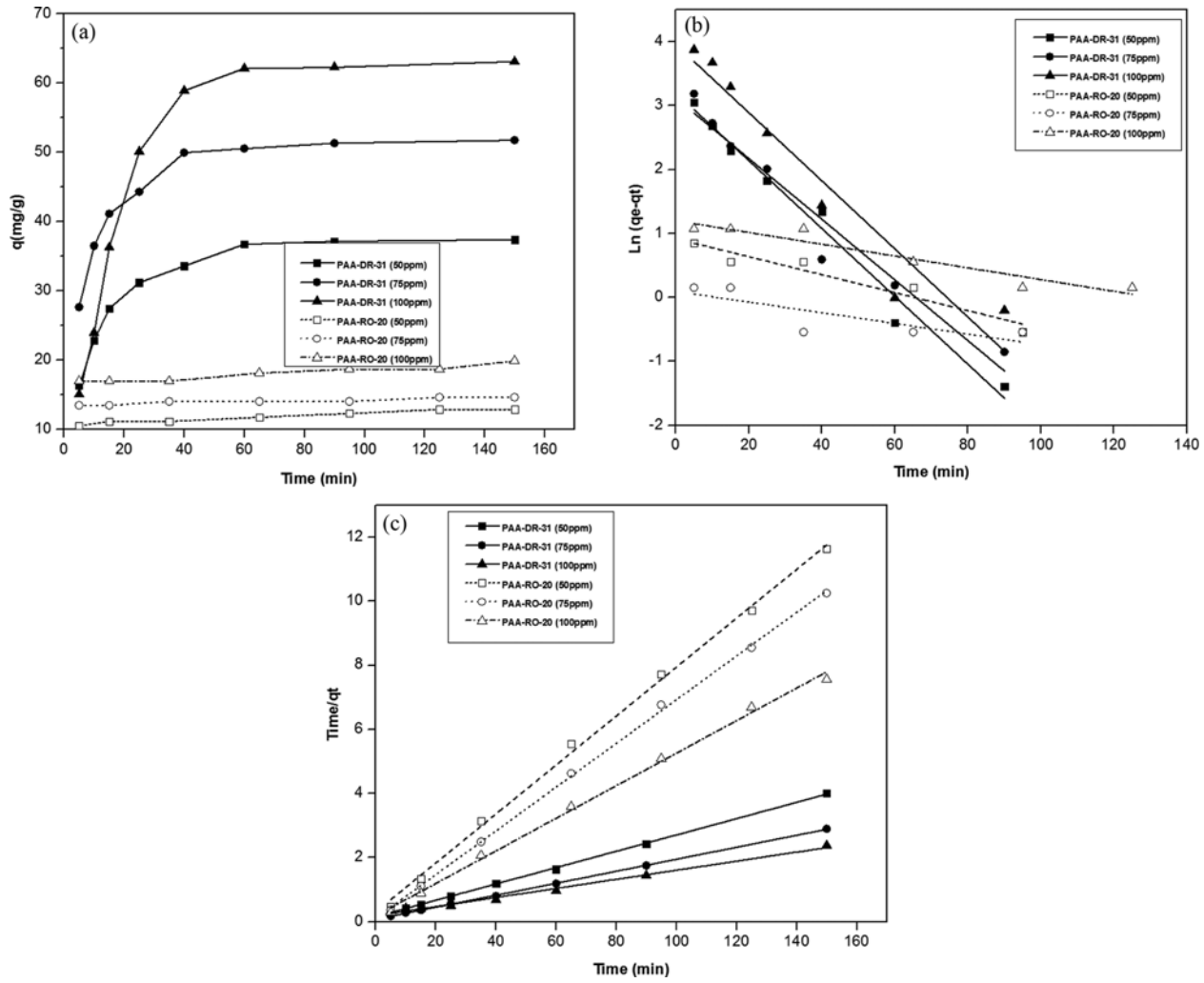

Fig. 11. Effect of contact time on the removal of DR-31 and RO-20 by PAA (a), pseudo-first-order model (b) pseudo-second-order model (c).

Table 3. Parameters of pseudo-first-order and pseudo-second-order kinetic models for adsorption of dyes onto PAM hydrogel

Concentration (mg/L)	$q_{e,exp}$ (mg/g)	Pseudo-first-order model			Pseudo-second-order model		
		$q_{e,cal}$ (mg/g)	k_1 (1/min)	R^2	$q_{e,cal}$ (mg/g)	k_2 (10^{-4}) (g/mg min^{-1})	R^2
D R-31 C=50 mg/L	43.06	34.156	0.035	0.983	47.058	15.85	0.9981
D R-31 C=75 mg/L	64.9	20.456	0.036	0.949	66.49	43.26	0.9999
D R-31 C=100 mg/L	81.28	73.405	0.044	0.991	88.96	8.99	0.9983
R O-20 C=50 mg/L	48.056	15.197	0.0313	0.989	49.14	55.27	0.9998
RO-20 C=75 mg/L	70.035	19.1727	0.0314	0.963	71.377	44.61	0.9998
RO-20 C=100 mg/L	92.4	26.81	0.026	0.992	94.34	27.88	0.9996

Table 4. Parameters of pseudo-first-order and pseudo-second-order kinetic models for adsorption of dyes onto PAA hydrogel

Concentration (mg/L)	$q_{e,exp}$ (mg/g)	Pseudo-first-order model			Pseudo-second-order model		
		$q_{e,cal}$ (mg/g)	k_1 (1/min)	R^2	$q_{e,cal}$ (mg/g)	k_2 (10^{-4}) (g/mg min^{-1})	R^2
D R-31 C=50 mg/L	37.383	24.49	0.0530	0.9783	39.32	39.51	0.9994
D R-31 C=75 mg/L	51.742	22.59	0.0474	0.9467	53.47	43.73	0.9997
D R-31 C=100 mg/L	63.092	52.05	0.0532	0.9136	70.72	10.35	0.9898
R O-20 C=50 mg/L	12.884	2.502	0.0140	0.9115	13.10	186.8	0.9975
RO-20 C=75 mg/L	14.628	1.098	0.0083	0.5499	14.67	413.0	0.9992
RO-20 C=100 mg/L	19.861	3.31	0.0092	0.8948	19.72	138.7	0.9966

onto PAM and PAA hydrogels and the adsorption data fitted well with Freundlich model for RO-20, indicating that a multilayer adsorption of RO-20 dye onto hydrogels.

2-4. Effect of Contact Time and Adsorption Kinetics Study

To determine the effect of contact time on the dye adsorption, 0.05 g of adsorbents was mixed with 50, 75 and 100 mg/L of dye solutions at room temperature. Figs. 10(a) and 11(a) show the plots of the q_e value of dyes for adsorption onto PAM and PAA versus the contact time at different initial dye concentrations. As seen, the adsorption capacity of RO-20 and DR-31 dyes increased rapidly with an increase of the contact time, then the rate of adsorption became slow and adsorption reached equilibrium. In the beginning, all active sites on the surface of adsorbents were vacant and then saturation occurred. The kinetics of RO-20 and DR-31 onto PAM and PAA were analyzed using pseudo-first order (Eq. (5)), pseudo-second order models (Eq. (6)) [33].

$$q_t = q_e(1 - e^{-K_1 t}) \quad (5)$$

$$q_t = \frac{K_2 q_e^2 t}{1 + K_2 q_e t} \quad (6)$$

where k_1 (1/min) and k_2 (g/mg min) are the rate constants of adsorption for the pseudo-first order and pseudo-second order models, q_e and q_t are the adsorption capacity of RO-20 or DR-31 at equilibrium and at time t (min). The linear fitting plots of pseudo-first and pseudo-second order models of PAM and PAA are given in Fig. 10(b), (c) and Fig. 11(b), (c), respectively. The kinetic parameters obtained from pseudo-first and pseudo-second order models are summarized in Tables 3 and 4. The results showed that the R^2 values for the pseudo-second order kinetic model of dyes were relatively higher than those from the pseudo-first order kinetic model. Also, the calculated q_e of dyes from the pseudo-second order model were in agreement with the experimental q_e of dyes. Therefore, the adsorptions of RO-20 and DR-31 onto PAM and PAA hydrogels are controlled by the chemisorption of dyes molecules.

A comparison of synthesized adsorbents in the present study with other materials for DR-31 removal is given in Table 5. To the best of our knowledge, there has been no report on the removal of RO-20 dye by other adsorbents so far. As can be seen, the PAM and PAA hydrogels are promising adsorbents for DR-31 and RO-20 dye adsorption from wastewater.

Table 5. Comparison of maximum adsorption capacity of DR-31 onto various adsorbents

Dye	Adsorbents	q_m (mg/g)	Refs.
DR-31	Activated carbon	111	[34]
	Rice husk	129.87	[35]
	Modified alginate	39.23	[36]
	PAM hydrogels	155.279	This work
	PAA hydrogel	143.884	This work

CONCLUSIONS

PAM and PAA hydrogels were prepared and their properties for removal of anionic dyes (RO-20 and DR-31 dyes) from aqueous solutions were investigated. Also, the adsorption efficiency of hydrogels was studied comparatively, and it was found that the PAM hydrogel had high adsorption capacity in comparison with PAA hydrogel. TGA analysis indicated that the thermal stability of PAM hydrogel was higher than the thermal stability of PAA hydrogel. The difference in the morphologies of hydrogels before and after dyes adsorption was confirmed by SEM analysis. Adsorption experiments were performed as function of pH, PAM or PAA dosage, contact time and initial dyes concentration. The optimum conditions for removal of DR-31 by PAM and PAA hydrogels were pH 3 and pH 1.5, exposure time of 90 and 60 minutes, respectively, initial dye concentration of 150 mg L^{-1} and hydrogel loading of 0.05 g. The optimum conditions for removal of RO-20 by PAM and PAA hydrogels were pH 3 and pH 2, exposure time of 95 and 65 minutes, respectively, initial dye concentration of 150 mg L^{-1} and hydrogel loading of 0.05 g. The adsorption capacity of dyes increased at low pH because of the strong electrostatic interaction between the positively charged adsorbents and the negatively charged RO-20 or DR-31 dyes. The adsorption of RO-20 and DR-31 dyes onto hydrogels agreed well to the Freundlich and Langmuir adsorption models, respectively. The kinetic study demonstrated that the adsorption process followed the pseudo-second-order kinetic model.

ACKNOWLEDGEMENTS

The authors are grateful for financial support from the Iran National Science Foundation Science deputy of presidency.

REFERENCES

1. M. Rafatullah, O. Sulaiman, R. Hashim and A. Ahmad, *J. Hazard. Mater.*, **70**, 177 (2010).
2. Z. Aksu, *Process Biochem.*, **40**, 997 (2005).
3. N. M. Mahmoodi, Z. Hosseinabadi-Farahani and H. Chamani, *Korean J. Chem. Eng.*, **33(3)**, 902 (2016).
4. A. Latif, S. Noor, Q. M. Sharif and M. Najeebullah, *J. Chem. Soc. Pak.*, **32**, 115 (2010).
5. Y. Xie, S. Li, G. Liu, J. Wang and K. Wu, *Chem. Eng. J.*, **192**, 269 (2012).
6. L. Lili, C. Xueling, W. Yuqing, L. Dawei and H. Dandan, *J. Taiwan. Inst. Chem. Eng.*, **44**, 67 (2013).
7. S. Wang, H. Li and L. Xu, *J. Colloid Interface Sci.*, **295**, 71 (2006).
8. P. Janos, H. Buchtova and M. Ryznarova, *Water Res.*, **37**, 4938 (2003).
9. L. R. Varghese, D. Das and N. Das, *Korean J. Chem. Eng.*, **33**(1), 238 (2016).
10. R. Dolphen, N. Sakkayawong, P. Thiravetyan and W. Nakbanpote, *J. Hazard. Mater.*, **145**, 250 (2007).
11. L. G. Yan, L. L. Qin, H. Q. Yu, S. Li, R. R. Shan and B. Du, *J. Mol. Liq.*, **211**, 1074 (2015).
12. A. T. Paulino, M. R. Guilherme, A. V. Reis, G. M. Campese, E. C. Muniz and J. Nozaki, *J. Colloid Interface Sci.*, **301**, 55 (2006).
13. N. Sahiner, S. Butun, O. Ozay and B. Dibek, *J. Colloid Interface Sci.*, **373**, 122 (2012).
14. H. I. Won, H. H. Nersisyan and C. W. Won, *Mater. Chem. Phys.*, **133**, 225 (2012).
15. N. Peppas, P. Bures, W. Leobandung and H. Ichikawa, *Eur. J. Pharm. Biopharm.*, **50**, 27 (2000).
16. M. A. Mekewi and A. S. Darwish, *Mate. Res. Bull.*, **70**, 607 (2015).
17. M. A. Mekewi, T. M. Madkour, A. S. Darwish and Y. M. Hashish, *J. Ind. Eng. Chem.*, **30**, 359 (2015).
18. S. Ghorai, A. Sinhamahpatra, A. Sarkar, A. Panda and S. Pal, *Bioresour. Technol.*, **119**, 181 (2012).
19. S. Zhou, A. Xue, Y. Zhao, Q. Wang, Y. Chen, M. Li and W. Xing, *Desalination*, **270**, 269 (2011).
20. R. Kunanuruksapong and A. Sirivat, *Mater. Sci. Eng. A.*, **454**, 453 (2007).
21. B. S. Kaith, R. Jindal, H. Mittal and K. Kumar, *Int. J. Polym. Mater.*, **61**, 99 (2012).
22. S. Li, H. Wang, W. Huang and X. Liu, *Colloid. Polym. Sci.*, **292**, 107 (2014).
23. S. Li, H. Zhang, J. Feng, R. Xu and X. Liu, *Desalination*, **280**, 95 (2011).
24. R. Bhattacharyya, S. Kumar Ray and B. Mandal, *J. Ind. Eng. Chem.*, **19**, 1191 (2013).
25. M. A. Malana, S. Ijaz and M. N. Ashiq, *Desalination*, **263**, 249 (2010).
26. C. Zhou, Q. Wu, T. Lei and I. I. Negulescu, *Chem. Eng. J.*, **251**, 17 (2014).
27. R. Bhattacharyya and S. Kumar Ray, *Chem. Eng. J.*, **260**, 269 (2015).
28. Y. H. Li, Q. J. Du, T. H. Liu, J. K. Sun, Y. Q. Jiao, Y. Z. Xia, L. H. Xia, Z. H. Wang, W. Zhang, K. L. Wang, H. W. Zhu and D. H. Wu, *Mater. Res. Bull.*, **47**, 1898 (2012).
29. I. Langmuir, *J. Am. Chem. Soc.*, **40**, 1361 (1918).
30. W. J. Weber and R. K. Chakravorti, *J. Am. Inst. Chem. Eng.*, **20**, 228 (1974).
31. M. K. Yoo, Y. K. Sung, Y. M. Lee and C. S. Cho, *Polymer*, **41**, 5713 (2000).
32. J. Koetz and S. Kosmella, *Polyelectrolytes and Nanoparticles*, Springer-Verlag Berlin Heidelberg (2007).
33. L. Lian, X. Cao, Y. Wu, D. Lou and D. Han, *J. Taiwan Inst. Chem. Eng.*, **44**, 67 (2013).
34. N. M. Mahmoodi, R. Salehi and M. Arami, *Desalination*, **272**, 187 (2011).
35. Y. Safa and H. N. Bhatti, *Desalination*, **272**, 313 (2011).
36. F. A. Khari, M. Khatibzadeh, N. M. Mahmoodi and K. Gharanjig, *Desalin Water Treat.*, **51**, 2253 (2013).